Progress In Electromagnetics Research C, Vol. 121, 97–106, 2022

A Triple Band C-Shape Monopole Antenna for Vehicle Communication Application

Dong Sik Woo*

Abstract—A compact triple band monopole antenna with a simple modified C-shape structure for vehicle-to-everything (V2X) application is presented. The proposed multiband vehicle antenna with three C-shaped round stubs structure satisfies the worldwide interoperability for microwave access (WiMAX), wireless local area network (WLAN), and wireless access in vehicular environment (WAVE) bands. The three resonant frequencies are implemented with three C-shaped round stubs, and they are simply controlled by adjusting the round stub length without influence each other. The presented antenna demonstrated good impedance bandwidth and nearly omnidirectional radiation patterns over the whole operating bands. The field communication tests by connecting the vehicular communication module were also performed and verified in the view of automotive vehicle antenna application.

1. INTRODUCTION

Recently, with the development of communication technologies such as 5G wireless communication, dedicated short range communication (DSRC), and Wi-Fi, research on high-reliability and low-latency autonomous vehicles that automatically recognize the driving environment and drive without a driver is being actively conducted. Vehicle-to-everything (V2X) is an essential technology for autonomous driving and has been standardized by DSRC in the US and cooperative intelligent transportation System (C-ITS) in Europe. Recently, mobile telecommunication operators have introduced and utilized cellular V2X (C-V2X), which is characterized by high reliability, short latency, and high data processing capacity. Also, researches on WAVE communication systems based on IEEE 802.11p MAC class using 5.85–5.925 GHz frequency bandwidth that provides vehicle to vehicle (V2V), pedestrian to vehicle (P2V), vehicle to infrastructure (V2I) in vehicle networking (IVN), and infrastructure to infrastructure (I2I) communication network functions are actively taking place in [1–7].

Modern automotive antennas are usually placed in a small space on car case. These automotive antenna modules like shark-fins contain antennas for GPS/GNSS navigation, DMB, digital audio broadcasting (DAB), emergency call (eCall), long-term evolution (LTE), Wi-Fi, WLAN, WiMAX, multiple-input multiple-output (MIMO) antennas for cellular systems, diversity antennas for V2X and satellite digital audio radio (SDARS). However, the antenna design suffers from limited space, the coupling between antennas, and shadowing of other radiation patterns due to a multitude of near-field effects. Also optimum positions are difficult to identify [8–15].

Several microstrip-feed and CPW-feed printed monopole antennas that can support WLAN and WiMAX applications, while potentially applicable as V2X vehicle antenna, have been reported and well designed to meet a dual or triple band operation [16–26]. In [27], two open ended inverted L-shaped slots on the radiation patch have been designed, but the slot position and dimension were ambiguous, and the E-plane radiation pattern was uneven. A compact triple band antenna for WLAN/WiMAX USB dongle

Received 2 June 2022, Accepted 24 June 2022, Scheduled 8 July 2022

* Corresponding author: Dong Sik Woo (dswoo@cu.ac.kr).

The author is with the School of Electronic and Electrical Engineering, Daegu Catholic University, 13-13 Hayangro, Gyeongsan-si, South Korea.

application with a circular-arc-shaped stub and an L-shaped stub is presented in [28]. However, due to the large coupling between adjacent stubs, the resonant frequencies are not independent of each other. In [29], by using a toothbrush-shaped patch (TSP), a meander line (ML), and an inverted U-shaped patch (IUSP), the three resonance frequencies are realized, but there are many design parameters, so the design is complicated, and optimization is difficult. In [30], a CPW-fed monopole antenna uses an L-shaped stub and a rectangle stub to cover 2.6–2.73 GHz, WiMAX and WLAN applications. However, the resonant frequencies cannot be tuned independently. The gain is relatively low, and the difference between the simulated and measured values is large. Fractal antennas can be a good alternative due to their self-similarity geometry that provides multiple resonances. They have I-shape, hexagonal shape, circular shape, and has the advantage of small size and high efficiency. The return loss and bandwidth are improved. However, it is observed that the design complexity and the limitation on the number of iterations for miniaturization lead to fabrication inaccuracies and take a lot of design time [31–35].

The design of a triple band monopole antenna with a C-shape structure is presented for WLAN, WiMAX, and WAVE band operations. Three resonant frequency bands were implemented through three different C-shaped round stubs. Compared to the previously reported antennas, the proposed antenna has a simple structure and has little influence on other resonant frequencies, so it can be designed independently. The change of the resonant frequency according to the length change of round stubs 1, 2, and 3 is investigated through parametric analysis. The designed antenna had good impedance bandwidth, relatively flat omnidirectional radiation patterns, and stable gain in the operating bands. Also, a simple field test using the integrated vehicle communication module is successfully performed.

2. ANTENNA DESIGN

The proposed triple band antenna is designed based on a multi-monopole antenna. The length of each round stub was designed in the desired frequency band to realize multiband characteristics, and the positions of each stub were appropriately placed. Fig. 1 shows the structure of the proposed antenna seen in the front and bottom views. Also, a microstrip transmission line with 50 Ω characteristic impedance was used as feed. The triple band C-shape antenna is printed on an FR4 substrate with thickness of 1 mm, relative dielectric constant (ε_r) of 4.6 in which the characteristic impedance Z_0 of the MSL was 50 Ω. The feed strip width of 1.8 mm and conductor thickness (t) 18 μm were used in the proposed antenna. The size of the antenna is about $24 \times 28\,\text{mm}^2$. The length of each C-shaped round stub (l_1, l_2, l_3) is about a quarter of the free space wavelength (λ_0) at the centre frequency of each band.

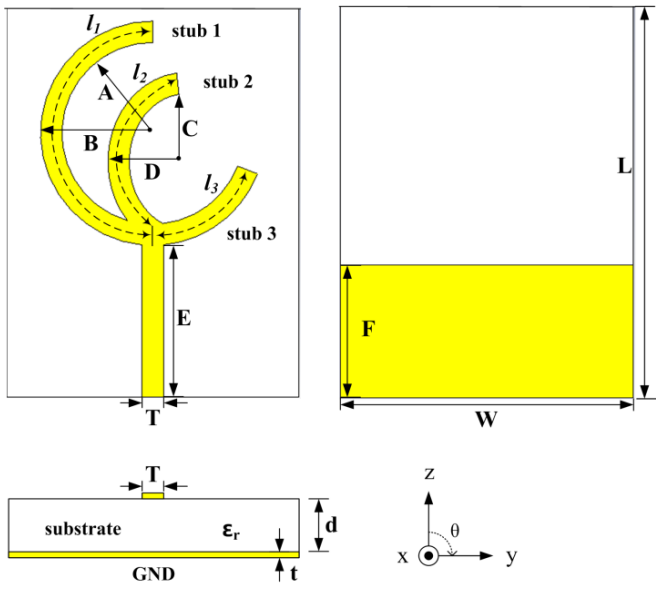

Figure 1. Configuration of proposed C-shape monopole antenna.

Therefore, the final value can be obtained by optimizing the length of each C-shape monopole. The optimized antenna parameters are listed as follows: $A = 8.2\,\text{mm}$, $B = 10\,\text{mm}$, $C = 7\,\text{mm}$, $E = 9.5\,\text{mm}$, $T = 1.8\,\text{mm}$, $L = 28\,\text{mm}$, $W = 24\,\text{mm}$, $d = 1\,\text{mm}$, $t = 0.018$, $l_1 = 30.6\,\text{mm}$, $l_2 = 16.6\,\text{mm}$, $l_3 = 11.1\,\text{mm}$.

3. PARAMETRIC ANALYSIS

The proposed antenna consists of C-shaped round stubs. Stub 1 resonates in WLAN band; stub 2 resonates in WiMAX band; and stub 3 resonates in WAVE band. The parametric studies and optimization of the proposed antenna are carried out by using HFSS by ANSYS, which is a commercial 3D electromagnetic simulation software. The design procedure of the proposed antenna is as follows:

1) First, the length of round stub 1 is adjusted to satisfy the WLAN band frequency;
2) Next, adjust the length of the round stub 3 of the antenna that can resonate in the WAVE band;
3) Finally, the proposed antenna design is completed by adding round stub 2 to form a resonant frequency in the WiMAX band. In this case, the position of the stubs is optimal to minimize engagement with round stubs 1 and 3.

3.1. Effect of Length Adjustment of Round Stub 1

Figure 2 shows the change in the S-parameters according to the change in the length of round stub 1. The line width W of stub 1 was 1.8 mm, which is the same as the width of the $50\,\Omega$ transmission line. It can be seen from Fig. 2 that the resonance frequency increases as the length of round stub 1 becomes shorter. Considering the combination effect with round stub 2, the optimal length of 30.6 mm of round stub 1 that satisfies the WLAN band (2.4–2.484 GHz) is selected. This corresponds to a quarter of the free space wavelength at 2.44 GHz. It is observed from the figure that the other two resonance frequencies are slightly changed. Therefore, it can be seen that round stub 1 determines the frequency of the WLAN band almost independently.

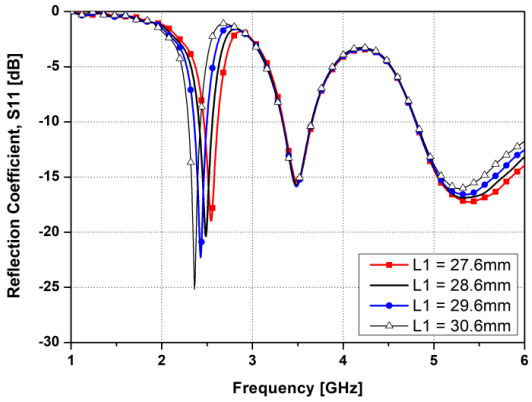

Figure 2. Simulated S-parameters according to change of length of the stub 1 (l_1).

3.2. Effect of Length Adjustment of Round Stub 2

In round stub 2, the line width W is the same as stub 1. An oval shape has been adopted for round stub 2 to minimizing the mutual coupling with the other two round stubs. Fig. 3 shows the change in the S-parameters according to the change in the length of round stub 2. The resonance frequency increases as the length of round stub 2 becomes shorter. At this time, the length was optimized to minimize the coupling between stub 1 and stub 3. A round stub 2 length of 16.6 mm that satisfies the WiMAX band (3.3–3.69 GHz) was used. It is optimized to be slightly shorter than a quarter of the free space wavelength at 3.5 GHz. As can be seen from the figure, the other two resonant frequencies do not change at all. Accordingly, it can be seen that round stub 2 determines only the frequency of the WiMAX band, and the mutual coupling is very small.

3.3. Effect of Length Adjustment of Round Stub 3

Figure 4 shows the simulated S-parameters according to the change in the length of round stub 3 after fixing to the optimized length of round stubs 1 and 2 derived above. It can be seen in Fig. 4 that the resonance frequency increases as the length of round stub 3 becomes shorter. In this case, the resonant frequency change according to the length change is rather large, and the other resonant frequencies also change slightly. Therefore, it can be seen that determining the length of round stub 3 first and then determining the length of round stub 2 is an effective way to design the entire triple band antenna. A round stub 3 length of 11.1 mm was chosen for the WAVE frequency band. This corresponds to a quarter of the free space wavelength at 5.9 GHz.

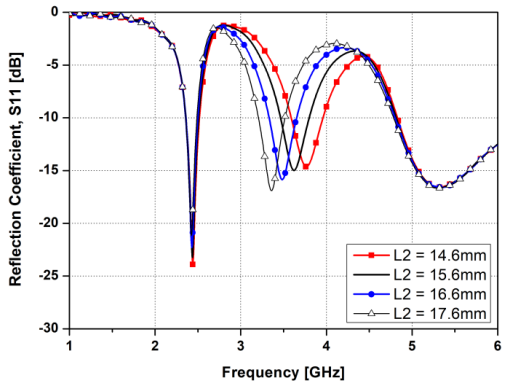

Figure 3. Simulated S-parameters according to change of length of the stub 2 (l_2).

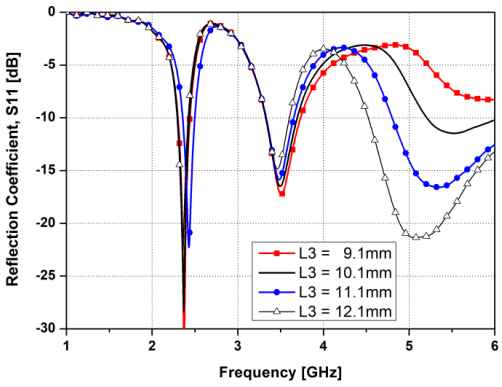

Figure 4. Simulated S-parameters according to change of length of the stub 3 (l_3).

4. FABRICATION AND MEASUREMENT RESULTS

4.1. Impedance Performance

In order to verify the overall performance, the proposed C-shape triple band antenna prototype is fabricated as shown in Fig. 5 and measured by utilizing the Anritsu 37397C vector network analyzer. Fig. 6 shows the simulated and measured S-parameters of the fabricated C-shape antenna. It can be seen that the proposed triple band antenna has three different resonance bands. The measured impedance bandwidths for $S_{11} < -10$ dB are about 210 MHz at WLAN band (2.34–2.55 GHz). In the WiMAX band (3.39–3.69 GHz), it has an operating frequency band of 300 MHz and 500 MHz at the WLAN/WAVE band (5.5–6.0 GHz) which fully cover the WLAN bands, WiMAX bands, and WAVE bands. However, due to fabrication tolerance and deterioration of characteristics because of connector connection, there was a slight discrepancy between the simulated and measured S-parameters. However, it sufficiently covers the 5.85–5.925 GHz IEEE 802.11p required by the WAVE/DSRC band.

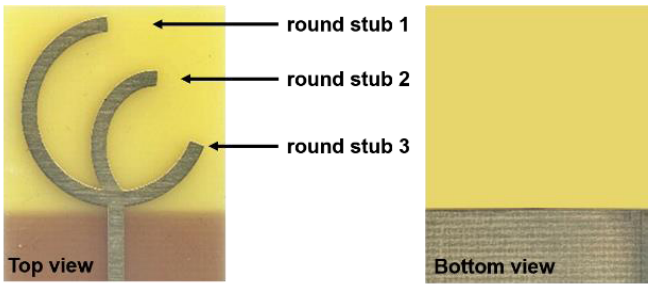

Figure 5. Fabricated proposed triple band C-shape antenna.

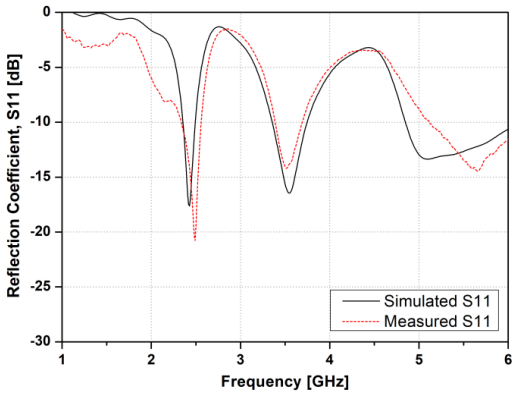

Figure 6. Simulated and measured reflection coefficient (S_{11}).

4.2. Radiation Performance

The radiation performance of the antenna was analyzed by measuring the radiation pattern and gain in the electromagnetic wave shielding room. A standard H-polarized antenna is utilized to measure the H-plane (x-y cut) radiation patterns, and an E-polarized standard horn antenna is utilized to measure the E-plane (z-y cut) radiation patterns. The rotation directions of the measuring the radiation patterns are in the ϕ and θ directions, respectively.

Figures 7(a), 8(a), and 9(a) show the radiation patterns in the H-plane measured in WLAN, WiMAX, and WAVE bands. Figs. 7(b), 8(b), and 9(b) show the radiation patterns in the E-plane measured in WLAN, WiMAX, and WAVE bands.

Figure 7 shows the radiation pattern in the WLAN band at 2.45 GHz. Nearly omnidirectional radiation patterns similar to that of a conventional monopole antenna appeared in the E-plane, and the peak gain was 2.3 dBi. It had similar characteristics to the simulation. Figs. 8 and 9 show the antenna radiation patterns for the WiMAX and WAVE bands, respectively. The E-plane also exhibited characteristics close to omnidirectional similar to that of a general monopole antenna, and the maximum gain was similar to those simulated at 2.6 dBi and 3.7 dBi, respectively.

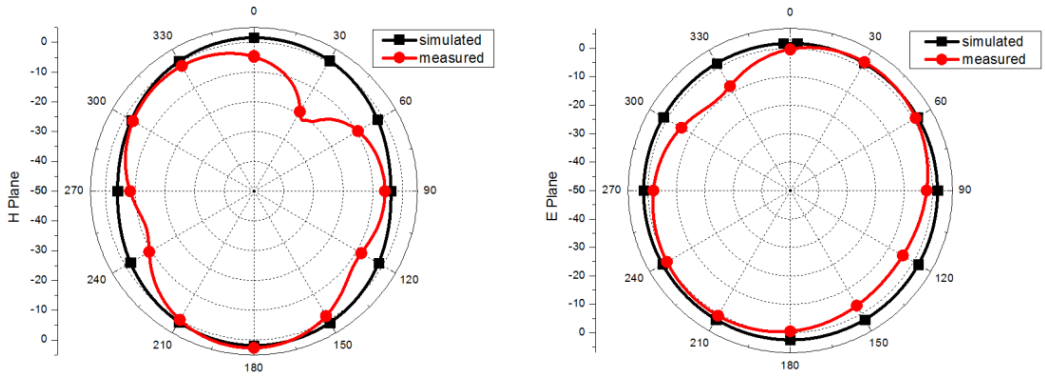

(a) (b)

Figure 7. Radiation patterns in the WLAN band: (a) H-plane (x-y cut); (b) E-plane (z-y cut).

4.3. Coupling Test Using Vehicle Communication Module

Coupling tests were performed using the V2X vehicle module for automotive communication systems operating in the WAVE frequency band. The coupling test setup using the vehicle communication module is shown in Fig. 10. The vehicle communication module is composed of a power supply unit, a

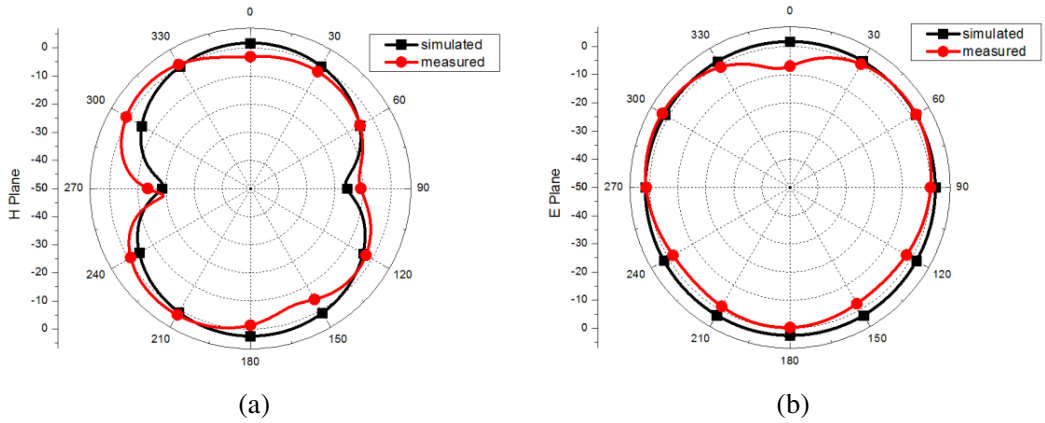

Figure 8. Radiation patterns in the WiMAX band: (a) H-plane (x-y cut); (b) E-plane (z-y cut).

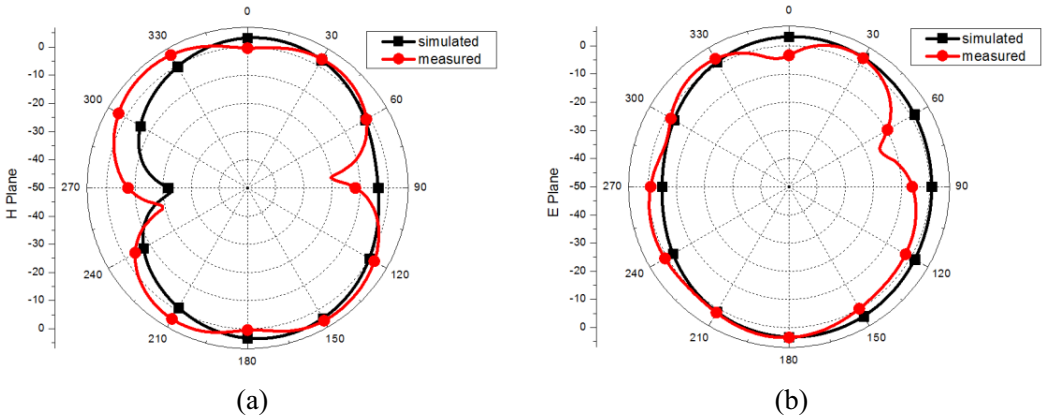

Figure 9. Radiation patterns in the Wave band: (a) H-plane (x-y cut); (b) E-plane (z-y cut).

Figure 10. Coupling test setup using vehicular communication module.

transmission unit, and a signal processing unit. The antenna used in the transmitter consists of a GPS antenna and a rod antenna, and a test was performed after replacing the rod antenna with the proposed antenna. Fig. 11 shows the result of communication test connected to the vehicle communication module. The developed vehicle communication module uses a commercial rod antenna. Firstly, after mounting the rod antenna, a transmission test was performed. Then, the proposed C-shape antenna was replaced, and the transmission test was performed once more. In Fig. 11, the signal level received

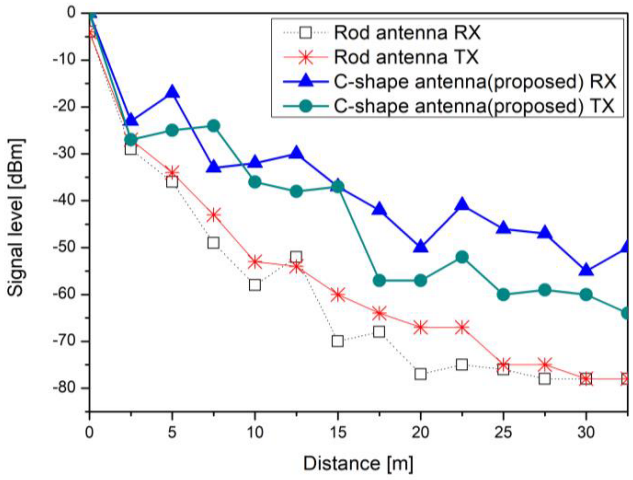

Figure 11. Comparison of measured signal levels between antennas.

from the vehicle communication module using both antennas was compared as a function of distance. It can be seen that the proposed C-shape antenna improved the receiver sensitivity by about 10 dB compared to the commercial rod antenna, and it was proved that it can be used as an antenna for a V2X communication system.

Table 1 compares the proposed antenna with previously reported other multiband antennas. It can be seen that the proposed antenna sufficiently covers the triple bands of 2.4/3.5/5.9 GHz. In addition, it has a smaller size and a simpler structure than the existing multiband antenna, and provides independent frequency tuning capability due to less interference between round stubs.

Table 1. Comparisons of some multiband antennas.

Ref.	Frequency bands [GHz]	Gain [dBi]	Size [mm^2]	Application
[26]	2.4/3.5/5.8	1.4/2.0/4.6	30×50	WLAN/WiMAX
[27]	2.45/3.45/5.5	1.8/1.9/2.4	10×29	WLAN/WiMAX
[28]	2.4/3.5/5.5	3.4/3.1/3.2	16×39	WLAN/WiMAX
[29]	2.4/3.5/5.5	1.3/2.2/3	20×30	WLAN/WiMAX
[30]	2.65/3.5/5.5	1.5/1.6/3.3	20×37	WLAN/WiMAX
[31]	3.9/5.4	0.4/−1.1	60×55	WiMAX/WLAN
This work	2.4/3.5/5.9	2.3/2.6/3.7	24×28	WLAN/WiMAX/WAVE

5. CONCLUSION

A design of a triple band C-shape antenna for autonomous driving V2X application is presented with an FR-4 substrate of overall size of 24×28 mm^2. The proposed antenna demonstrated good impedance and radiation characteristics in the desired WLAN (2.4 GHz), WiMAX (3.5 GHz), WLAN (5.2–5.8 GHz), and WAVE (5.9 GHz) frequency bands. The lengths of three round stubs, which are the main design parameters of the triple band C-shape antenna, can be independently designed in each frequency band, and it has been proven that the influence of each other is insignificant. The measured peak gains were 2.3 dBi, 2.6 dBi, and 3.7 dBi, respectively. As a result of compatibility and coupling tests with the vehicle communication module, it was found that the receiver signal sensitivity was improved by about 10 dB compared to the commercial rod antenna. Therefore, the proposed antenna is small enough to be built in a narrow space or curved surface of automotive vehicle, and can be used as a multiband

antenna by mounting it on another vehicle or road-side unit (RSU) for C-ITS application. Or, it will be widely used by mounting it on drones, wireless communication sensors, and wearable devices.

ACKNOWLEDGMENT

This work was supported by research grants from Daegu Catholic University in 2021 (No. 20213016).

REFERENCES

1. Artner, G., W. Kotterman, G. Del Galdo, and M. A. Hein, "Automotive antenna roof for cooperative connected driving," *IEEE Access*, Vol. 7, 20083, 2019, DOI: 10.1109/ACCESS.2019.2897219.
2. Varum, T., J. N. Matos, P. Pinho, and A. Oliveira, "Printed antenna for DSRC systems with omnidirectional circular polarization," *IEEE Int. Conf. on Intelligent Transportation Systems*, 475–478, 2012, DOI: 10.1109/ITSC.2012.6338677.
3. Wu, Q., Y. Zhou, and S. Guo, "An L-sleeve L-monopole antenna fitting a shark-fin module for vehicular LTE, WLAN, and car-to-car communications," *IEEE Trans. on Vehicular Technology*, Vol. 67, 7170–7180, 2018, DOI: 10.1109/TVT.2018.2828433.
4. Erlacher, F., F. Klingler, C. Sommer, and F. Dressler, "On the impact of street width on 5.9 GHz radio signal propagation in vehicular networks," *Con. on WONS*, 143–146, 2014, DOI: 10.1109/WONS.2014.6814735.
5. Hua, Y., L. Huang, and Y. Lu, "A compact 3-port multiband antenna for V2X communication," *IEEE Int. Symp. on Ant. and Propag. & USNC/URSI*, 639–640, 2017, DOI: 10.1109/APUSNCURSINRSM.2017.8072362.
6. Yaqub, M. A., S. H. Ahmed, and D. Kim, "Asking neighbors a favor: Cooperative video retrieval using cellular networks in VANETs," *Vehicular Communications*, Vol. 12, 39–49, 2018, DOI: https://doi.org/10.1016/j.vehcom.2017.12.002.
7. Kumar, O. P., P. Kumar, T. Ali, P. Kumar, and S. Vincent, "Ultrawideband antennas: Growth and evolution," *Micromachines*, Vol. 13, 60, 2022, DOI: https://doi.org/10.3390/mi13010060.
8. Sahar, N. M., M. T. Islam, and N. M. Misran, "A reconfigurable multiband antenna for RFID and GPS applications," *Elektronika Ir Elektrotechnika*, Vol. 21, 44–50, 2015, DOI: https://doi.org/10.5755/j01.eee.21.6.13760.
9. Goncharova, I. and S. Lindenmeier, "Compact satellite antenna module for GPS, Galileo, GLONASS, BeiDou and SDARS in automotive application," *IET Microw., Antennas Propag.*, Vol. 12, 445, 2018, DOI: 10.1049/iet-map.2017.0598.
10. Chiu, T.-L., L. Huitema, O. Pajona, and T. Monediere, "Compact and multiband MIMO dielectric resonator antenna for automotive LTE communications," *Int. J. Antennas and Propag.*, Article ID 8231081, 2018, DOI: https://doi.org/10.1155/2018/8231081.
11. Liou, C.-Y. and S.-G. Mao, "Miniaturized shark-fin rooftop antenna with integrated DSRC communication module for connected vehicles," *Symp. Int. URSI GASS*, 1–4, 2017, DOI: 10.23919/URSIGASS.2017.8105291.
12. Cheng, Y., J. Lu, and C. Wang, "Design of a multiple band vehicle-mounted antenna," *Int. J. Antennas and Propag.*, Article ID 6098014, 2019, DOI: https://doi.org/10.1155/2019/6098014.
13. Kim, I., S. Lee, and J. Lee, "Triple-band uniform circular array antenna for a multi-functional radar system," *Electronics*, Vol. 10, 2021, 1488, DOI: https://doi.org/10.3390/electronics10121488.
14. Mallahzadeh, A., A. Sedghara, and S. M. A. Nezhad, "A Tunable multi-band meander line printed monopole antenna for MIMO systems," *Proc. EUCAP*, 315–318, 2011.
15. Diez, M. B., P. Plitt, W. Pascher, and S. Lindenmeier, "Antenna placement and wave propagation for Car-to-Car communication," *Proc. Eur. Microw. Conf. (EuMC)*, 207–210, 2015, DOI: 10.1109/EuMC.2015.7345736.
16. Lu, J.-H. and Y.-H. Li, "Planar multi-band T-shaped monopole antenna with a pair of mirrored L-shaped strips for WLAN/WiMAX operation," *Progress In Electromagnetics Research C*, Vol. 21, 33–44, 2011.

17. Mehdipour, A., A. Sebak, C. W. Trueman, and T. A. Denidni, "Compact multiband planar antenna for 2.4/3.5/5.2/5.8-GHz wireless applications," *IEEE Ant. and Wireless Propag. Letters*, Vol. 11, 144–147, 2012, DOI: 10.1109/LAWP.2012.2185915.
18. Zhai, H., Z. Ma, Y. Han, and C. Liang, "A compact printed antenna for triple-band WLAN/WiMAX applications," *IEEE Ant. and Wireless Propag. Letters*, Vol. 12, 65, 2013, DOI: 10.1109/LAWP.2013.2238881.
19. Ellis, S. M., Z. Zhao, J. Wu, Z.-P. Nie, and Q. H. Liu, "A new compact microstrip-fed monopole antenna for triple band WLAN/WiMAX applications," *Progress In Electromagnetics Research Letters*, Vol. 48, 129–135, 2014.
20. Moosazadeh, M. and S. Kharkovsky, "Compact and small planar monopole antenna with symmetrical L- and U-shaped slots for WLAN/WiMAX applications," *IEEE Ant. and Wireless Propag. Letters*, Vol. 13, 388–391, 2014, DOI: 10.1109/LAWP.2014.2306962.
21. Yang, X., X. Liu, and C. Song, "A triple-band monopole planar antenna for WLAN and WiMAX applications," *Frequenz*, Vol. 69, 305–309, 2015, DOI: https://doi.org/10.1515/freq-2014-0153.
22. Li, L., X. Zhang, X. Yin, and L. Zhou, "A compact triple-band printed monopole antenna for WLAN/WiMAX applications," *IEEE Ant. and Wireless Propag. Letters*, Vol. 15, 1853–1855, 2016, DOI: 10.1109/LAWP.2016.2539358.
23. Gautam, A. K., L. Kumar, B. K. Kanaujia, and K. Rambabu, "Design of compact F-shaped slot triple-band antenna for WLAN/WiMAX applications," *IEEE Trans. Ant. and Propag.* Vol. 64, 1101–1105, 2016, DOI: 10.1109/TAP.2015.2513099.
24. Nandi, S. and A. Mohan, "CRLH unit cell loaded triband compact MIMO antenna for WLAN/WiMAX applications," *IEEE Ant. and Wireless Propag. Letters*, Vol. 16, 2017, 1816–1819, DOI: 10.1109/LAWP.2017.2681178.
25. Surendrakumar, P. and B. C. Mohan, "A triple-frequency, vertex-fed antenna for WLAN/WiMAX applications," *IEEE Ant. and Propag. Magazine*, Vol. 60, 101–106, 2018, DOI: 10.1109/MAP.2018.2818007.
26. Luo, C.-M., J.-S. Hong, and M. Amin, "A decoupling method between two tri-band antennas for WLAN/WiMAX applications," *IEICE Electron. Express*, Vol. 14, 20170354, 2017, DOI: https://doi.org/10.1587/elex.14.20170354.
27. Zheng, Y., P. Wang, M. Hua, and P. Gao, "Compact triple-band monopole antenna for WLAN/WiMAX applications," *IEICE Electron. Express*, Vol. 10, 20130638, 2013, DOI: https://doi.org/10.1587/elex.10.20130638.
28. Shi, Y. W., L. Xiong, and M. G. Chen, "Compact triple-band monopole antenna for WLAN/WiMAX-band USB dongle applications," *ETRI Journal*, Vol. 37, 21–25, 2015, DOI: https://doi.org/10.4218/etrij.15.0114.0676.
29. Li, Y. and W. Yu, "A miniaturized triple band monopole antenna for WLAN and WiMAX applications," *Int. J. Antennas and Propag.*, Article ID 146780, 2015, DOI: https://doi.org/10.1155/2015/146780.
30. Manouare, A. Z., S. Ibnyaich, A. E. Idrissi, A. Ghammaz, and N. A. Touhami, "A compact dual-band CPW-fed planar monopole antenna for 2.62–2.73 GHz frequency band, WiMAX and WLAN applications," *J. Micr. Opto. and Elec. App.*, Vol. 16, 564, 2017, DOI: https://doi.org/10.1590/2179-10742017v16i2911.
31. Ez-Zaki, F., A. Ghammaz, and H. Belahrach, "Multiband fractal antenna for wireless applications," *2018 6th International Conference on Wireless Networks and Mobile Communications (WINCOM)*, 1–6, 2018, DOI: 10.1109/WINCOM.2018.8629615.
32. Hong, T., S. Gong, Y. Liu, and W. Jiang, "Monopole antenna with quasi-fractal slotted ground plane for dual-band applications," *IEEE Ant. and Wire. Propag. Lett.*, Vol. 9, 595–598, 2010, DOI: 10.1109/LAWP.2010.2053834.
33. Viani, F., M. Salucci, F. Robol, and A. Massa, "Multiband fractal ZigBee/WLAN antenna for ubiquitous wireless environments," *J. of Elec. Waves. and Appl.*, Vol. 26, 1554–1562, 2012, DOI 10.1080/09205071.2012.704553.

34. Salucci, M., N. Anselmi, S. Goudos, and A. Massa, "Fast design of multiband fractal antennas through a system-by-design approach for NB-IoT applications," *EURASIP Journal on Wireless Communications and Networking*, 68, 2019, DOI: 10.1186/s13638-019-1386-4.
35. Akkole, S. and N. Vasudevan, "Compact multiband microstrip fractal antenna design for wireless applications — An overview," *2020 4th Int'l. Conf. on Elec. Com. and Aero Tech (ICECA)*, 2020, DOI: 10.1109/ICECA49313.2020.9297629.